Volume 6, Number 2 (April 2013) p. 211-226 • ISSN 1983-4195

REVISTA IBRACON DE ESTRUTURAS E MATERIAIS

IBRACON STRUCTURES AND MATERIALS JOURNAL

Numerical analysis of reinforced concrete beams strengthened with high strength cement-based composite material

Análise numérica de vigas de concreto armado reforçadas por compósitos formados por fibras de alta resistência e argamassa de cimento



C. M. PALIGA [a]
charlei.paliga@ufpel.edu.br

M. V. REAL [b]
mauroreal@furg.br

A. CAMPOS FILHO [c]
americo@ufrgs.br

Abstract

The use of composite materials based on polymeric resins and fiber as strengthening in concrete structures has been widely used. The use of carbon fiber reinforced polymers or other synthetic fibers is consolidated by its excellent characteristics, such as high strength, low weight, corrosion resistance, etc. This material in the form of sheets or laminates is bonded to the concrete substrate with epoxy-based adhesives. Although epoxy has proven to have excellent bonding and resistance performance, it has some disadvantages, such as low permeability, poor thermal compatibility with the base concrete, poor fire resistance, etc. Cement-based composite systems consisting of FRPs and a cementitious bonding agent can be used to prevent some of these problems. This study presents the numerical analysis, using a non-linear finite element model, of the structural behavior of reinforced concrete beams externally reinforced with a composite material made of high-strength synthetic fiber mesh and cementitious mortar. The numerical results were compared with experimental results reported in international journals, demonstrating the efficiency of the strengthening technique and the numerical model capacity.

Keywords: numerical analysis, ultra-high strength fiber meshes, cementitious mortar, structural strengthening.

Resumo

A aplicação de materiais compósitos à base de resinas poliméricas e fibras no reforço de estruturas de concreto armado se tornou uma técnica bastante difundida nos últimos tempos. O uso dos compósitos reforçados com fibras de carbono, ou outros tipos de fibras sintéticas, se consolidou pelas suas excelentes características, tais como elevada resistência, baixo peso, resistência à corrosão, etc. Este material, na forma de lâminas ou laminados, é colado no substrato de concreto através de adesivos à base de epóxi. Apesar do uso do epóxi apresentar excelentes resultados em termos de colagem e resistência, algumas desvantagens podem ser citadas, tais como: baixa permeabilidade, baixa compatibilidade térmica em relação ao concreto, baixa resistência ao fogo, etc. Para evitar alguns desses problemas, um sistema compósito à base de tecidos ou malhas de fibras sintéticas coladas na superfície de concreto com argamassa de cimento pode ser usado. O objetivo deste trabalho é fazer uma análise numérica, através de um modelo não linear de elementos finitos, do comportamento estrutural de vigas de concreto armado reforçadas à flexão com compósitos baseados na combinação de tecidos de fibras sintéticas de alta resistência e argamassa de cimento. Os resultados numéricos são comparados aos resultados experimentais publicados em artigos técnicos internacionais, que demonstram a eficiência da técnica de reforço e a capacidade do modelo numérico.

Palavras-chave: análise numérica, fibras de alta resistência, argamassa de cimento, reforço estrutural.

[a] *Universidade Federal de Pelotas, Departamento de Tecnologia da Construção, charlei.paliga@ufpel.edu.br, Rua Benjamin Constant 1359, Pelotas/RS, Brasil;*
[b] *Universidade Federal do Rio Grande, Escola de Engenharia, mauroreal@furg.br, Av. Itália km 8, Campus Carreiros, Rio Grande/RS, Brasil;*
[c] *Universidade Federal do Rio Grande do Sul, PPGEC, americo@ufrgs.br, Av. Osvaldo Aranha 99 – 3º andar, Porto Alegre/RS, Brasil.*

Received: 06 Sep 2012 • Accepted: 24 Oct 2012 • Available Online: 05 Apr 2013

1. Introduction

Composite materials based on high-strength synthetic fibers have been widely employed to strengthen and rehabilitate reinforced concrete structures in the last few years due to their excellent properties, including low weight, high mechanical strength, high resistance to corrosion, etc. Fiber-reinforced polymers are available as sheets or laminates bonded to reinforced concrete structures by epoxy-based bonding agents, improving their structural performance both under service conditions and ultimate loads.

Although epoxy-based bonding agents may present excellent concrete bonding and mechanical strength, their use also poses some problems. Epoxy resins have low permeability, low thermal compatibility with concrete, low fire resistance, and high susceptibility to ultraviolet radiation. Some of these problems may be prevented using a composite system based in synthetic fiber fabric or laminate bonded to the concrete surface by cement mortar. These systems can have different solutions, such as textile reinforced concrete (TRC), textile reinforced mortar (TRM), fiber reinforced concrete (FRC), and fiber reinforced cementitious mortar (FRCM). Di Tommaso et al. [2] and Aiello et al. [3] analyzed the behavior of reinforced concrete beams externally strengthened with FRCM consisting of carbon-fiber fabric in a cement matrix. The results showed that the composite system was efficient in terms of strength, stiffness, and ductility. The FRCM system was recently improved by the use of polypara-phenylene-benzo-bisthiazole (PBO) fiber fabric. The mechanical properties of PBO fibers are much better than those of the most resistant carbon fibers (Ombres [1]). In addition, they have high tolerance to impact, better energy absorption capacity than other fibers, as well as high resistance to fire and are chemically compatible with cement mortars (Wu et al. [4]).

The use of PBO fiber fabrics (see Figure 1) in FRCM systems is still being investigated. Tests with concrete beams reinforced with PBO fabric bonded to concrete using cement mortar (PBO-FRCM) were recently carried out. Experimental analyses with CFRP (carbon fiber reinforced polymers) bonded with epoxy resin and PBO-FRCM to reinforce concrete beams were performed by Di Tommaso et al. [5]. The following results were obtained: (i) flexure failure of the beams strengthened with PBO-FRCM was more ductile than CFRP-strengthened beams due to a gradual loss in composite action caused by the slipping of fibers/cementitious mortar; (ii) in PBO-FRCM strengthened beams, failure mechanisms related to the loss of strengthening action (debonding) are determined by the concrete/cementitious mortar interface, whereas in CFRP strengthened beams, failure due to debonding is determined by shearing of the concrete cover layer; and (iii) PBO-FRCM has also shown efficient as strengthening against shear of reinforced concrete beams.

Figure 1 – PBO fabric mesh

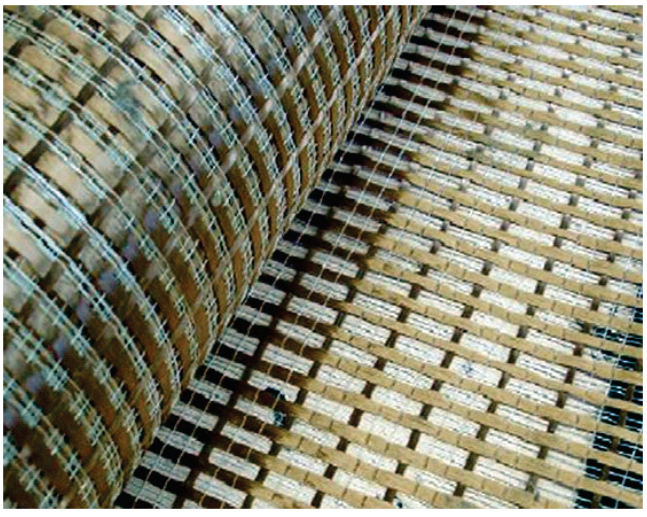

Figure 2 – Longitudinal and cross section of the beams tested by Ombres (1)

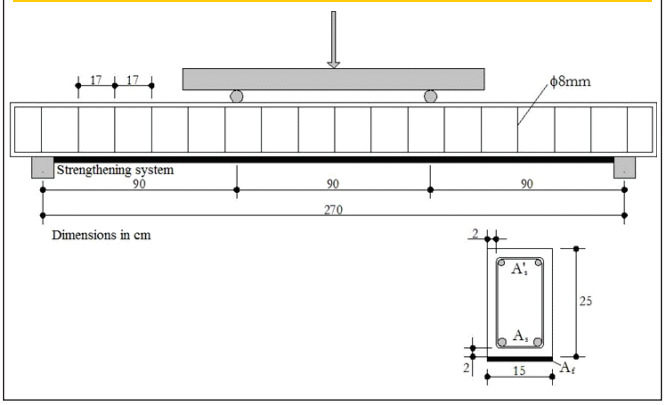

The objective of the present study was to perform a numerical analysis of concrete beams strengthened with this new material (PBO-FRCM) relative to flexural strength. The numerical model is based on the finite element method, and it may follow up the response of the evaluated structure from initial loading to failure load. The model can also predict failures modes, including ductile – due to excessive elongation of the tension reinforcement or to rupture of the strengthening system – and fragile – due to concrete crushing or strengthening system debonding – failures. The numerical data were compared with the experimental results obtained by Ombres [1], demonstrating both the efficacy of the strengthening material and the potentials of the numerical model.

2. Tested beam characteristics

Flexural strength of the simply supported beams was tested with two loads concentrated at 90cm from the bearing supports. Beam span was 270cm between supports, and beams presented 15x25cm rectangular cross section (Figure 2). Two beam series, designated as S_1 and S_2, were tested. In series S_1, the tensioned reinforcement, As, consisted of three 12mm bars (3ø12mm), whereas the compressed reinforcement, A's, consisted of two 10mm bars (2ø10mm). In series S_2, the tensioned reinforcement consisted of two 10mm bars (2ø10mm), whereas two 8mm bars (2ø8mm) where used in the compressed reinforcement. In order to prevent beam shear failures, 8mm stirrups placed every 17cm were used (ø8c.17). The beams were strengthened with one, two,

Table 1 – Mechanical properties of PBO fabric mesh and cementitious mortar

	Nominal thickness (mm)	Elastic modulus (GPa)	Tensile strength (MPa)	Tensile strain (‰)	Compression strength (MPa)
PBO fiber mesh	0.0455 (longitudinal) 0.0224 (transversal)	270	5,800	21.5	-
Mortar	-	6	3.5	-	29

Table 2 – Amount of internal reinforcement and strengthening in each series

Beam serie	Number of strengthening layers	A_s (mm^2)	A'_s (mm^2)	A_f (mm^2)	ρ_s (%)	ρ_f (%)
S_1	1	339.30	157.00	6.75	0.905	0.018
	1	339.30	157.00	6.75	0.905	0.018
S_2	1	157.00	100.53	6.75	0.419	0.018
	2	157.00	100.53	13.50	0.419	0.036
	3	157.00	100.53	20.25	0.419	0.054

or three 15cm-wide PBO-FRCM layers. The mechanical properties of the PBO fabric are presented in Table 1.

Table 2 shows tensile reinforcement ratio, compression ratio, and PBO fibers reinforcement ratio of each series.

During the process of beam manufacturing, curing was performed at environmental temperature, and the prototypes were strengthened 30 days after concrete placement. In order to ensure good bonding conditions between concrete and the mortar substrate, the beams were sandblasted to remove cement powder, washed with water, and left to dry at environmental temperature for a few days. After the first mortar layer was applied on the concrete substrate, the first layer of PBO fabric was applied and slightly pressed inside the mortar. A second mortar layer was then applied to completely cover the PBO fabric, and this operation was repeated until all PBO fabric layers were applied and covered with mortar (Ombres [1]).

Concrete mechanical properties were determined after at least 28 days of concrete placement using cubic or cylindrical test specimens. Mean compressive strength, f_{cm}, tensile strength, f_{tm}, and elastic modulus, E_{cm}, values are presented in Table 3. The same table shows mean yield strength values of the internal reinforcement, which were determined in standardized specimen tests (at least three per diameter).

3. Finite element numerical model

3.1 Model for concrete

Concrete is represented by two-dimensional isoparametric eight-node finite elements for plane stress state. The constitutive two-dimensional model for concrete is based on the model proposed by Darwin and Pecknold [6] employing the equivalent uniaxial strain and the two-dimensional failure criterion of Kupfer and Gerstle [7]. For the tensioned concrete after cracking, a curve that includes softening was adopted to take into account concrete contribution to tension-stiffening between cracks.

3.2 Model for steel

Reinforcement is represented by the embedded model, based on the study of Elwi and Hrudey [8]. Each reinforcement bar was considered

Table 3 – Materials properties

Beam serie	f_{cm} (MPa)	f_{tm} (MPa)	E_{cm} (MPa)	Internal reinforcement diameter (mm)	f_{ym} (MPa)
S_1	22.77 (c.o.v=4.38%)	2.03	28,140	12	515.44
				10	521.89
S_2	23.02 (c.o.v=6.70%)	2.12	28,160	10	525.90
				8	535.60

Figure 3 – Constitutive model for the interface concrete/strengthening system

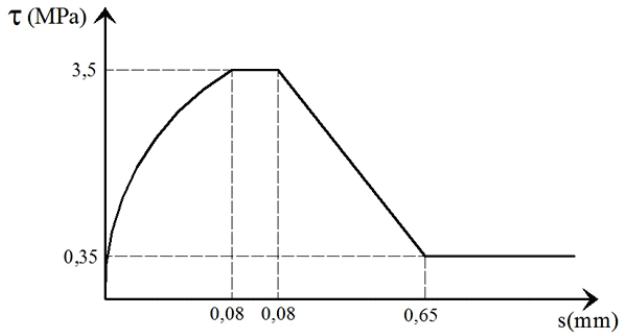

as a stiffer line inside the concrete that resists only to axial forces. It was assumed perfect bonding between the reinforcement and the concrete that involves it. Therefore, the reinforcement stiffness matrix has the same dimensions as the concrete element. The adopted steel constitutive equation is bilinear both for tension and compression.

3.3 Model for the strengthening composite material

The strengthening material was modeled by quadratic elements of plane truss with three nodes. The element is fixed to the remaining finite element mesh by an interface element. These materials are modeled as having linear elastic behavior until rupture stress is achieved, and are able to absorb only tension forces parallel to their longitudinal axis.

3.4 Model for the interface between the concrete substrate and the PBO- FRCM system

The transference of forces between the external strengthening system and the concrete generates bond stresses at the interface between the two materials. These stresses may lead to the premature debonding of the PBO-FRCM system and consequent structure failure with little mobilization of its resistance capacity, indicating that the material was underutilized. Slipping between reinforcement and concrete was calculated using a six-node one-dimensional interface element with quadratic interpolation functions, according to Adhikary and Mutsuyoshi [9]. The constitutive model applied is that recommended by the CEB-FIP Model Code 1990 [10], with bond stress (τ) to slip (s) relationship parameters obtained by Silva [11] and shown in Figure 3.

3.5 Finite element mesh used for numerical analyses

Due to the loading symmetry, mechanical properties, and geometry, only half of the beams were used in the numerical simulations. The finite element mesh used in the numerical simulations is presented in Figure 4. Concrete was discretized by 18 two-dimensional plane stress elements, and the external reinforcement and the interface concrete/strengthening were discretized by eight one-dimensional elements.

Further details of the finite element model used in the numerical simulations are described by Paliga et al. [12].

4. Results

In this section, the results obtained using numerical simulations are presented, discussed and compared with the results of the experimental program (Ombres[1]). It must be mentioned that the finite element model was able to follow up beam performance from initial loading to ultimate load. The numerical model was also able to detect beam failure mode. Failure may be ductile, due to excessive elongation of the tensioned reinforcement or to failure caused by PBO-FRCM material tension, or fragile, resulting from crushing of the compressed concrete or from PBO-FRCM system debonding.

4.1 Series S_1

In this series, two beams were reinforced at a tension reinforcement

Figure 4 – Finite elements mesh

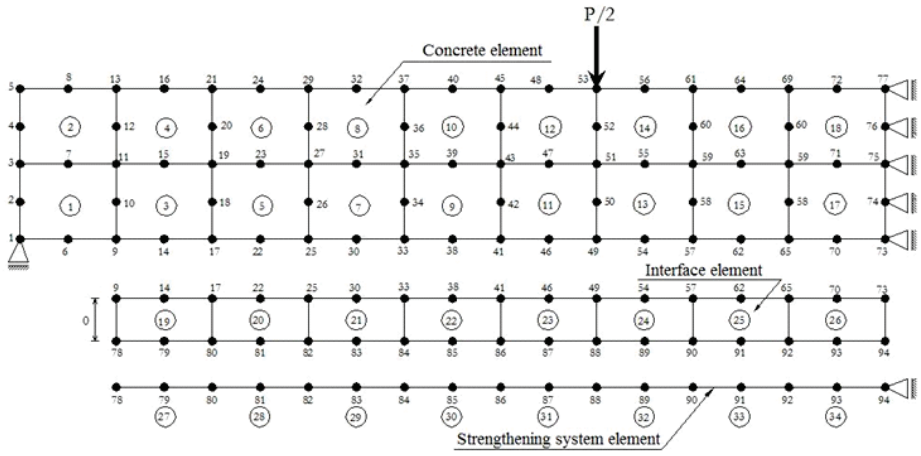

Figure 5 – Load-deflection curves (node 73 – Figure 4) for Beam Serie S_1

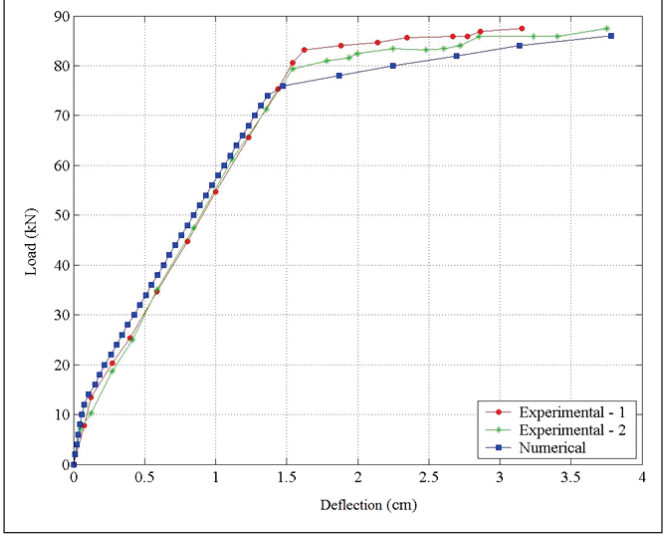

ratio of 0.905% (3ø12mm), compression ratio of 0.419% (2ø10mm) and strengthening ratio of 0.018% (a 6.75mm² layer). According to Ombres [1], rupture load of the first prototype was 87.42kN, and failure was caused by concrete crushing. The second prototype failed also due concrete crushing at 87.60kN ultimate load. The rupture load obtained by the numerical model was 86.25kN, representing an average difference of -1.4% relative to the experimental values.
Figure 5 shows the load-deflection curves obtained experimentally, which are compared with the beam performance numerically calculated.

Figure 6 shows the comparison between the experimental and the numerical values for concrete compressive strain (sample point near node 77) and for maximum strengthening tensile strain (sample point near node 94).

4.2 Series S_2

In this series, three numerically simulated beams were reinforced with a tension reinforcement ratio of 0.419% (2ø10mm), compression ratio of 0.268% (2ø8mm) and PBO-FRCM reinforcement ratio of 0.018% (one 6.75mm² layer), 0.036% (two 13.5mm² layers) and 0.054% (three 20.25mm² layers).

4.2.1 Beam strengthened with one PBO-FRCM layer

According to Ombres [1], the beam strengthened with one PBO-FRCM layer failed at a 54.24kN load due to concrete crushing. The rupture load numerically obtained by finite element model was 52.25kN, representing a difference of -3.7% relative to the experimental value.
Figure 7 shows the load-deflection curves obtained experimentally and numerically.
Figure 8 shows the comparison between the experimental and the numerical values for concrete compressive strain (sample point near node 77) and for maximum strengthening tensile strain (sample point near node 94).

4.2.2 Beam strengthened with two PBO-FRCM layers

According to Ombres [1], the beam strengthened with two PBO-FRCM layers collapsed at a 66.00kN load due to the debonding of the strengthening system from the concrete substrate. The rupture load numerically obtained by finite element model was 68.75kN, representing a difference of +4.2% relative to the experimental value.

Figure 6 – Load versus Strain in the mid-span section for Beam Serie S_1

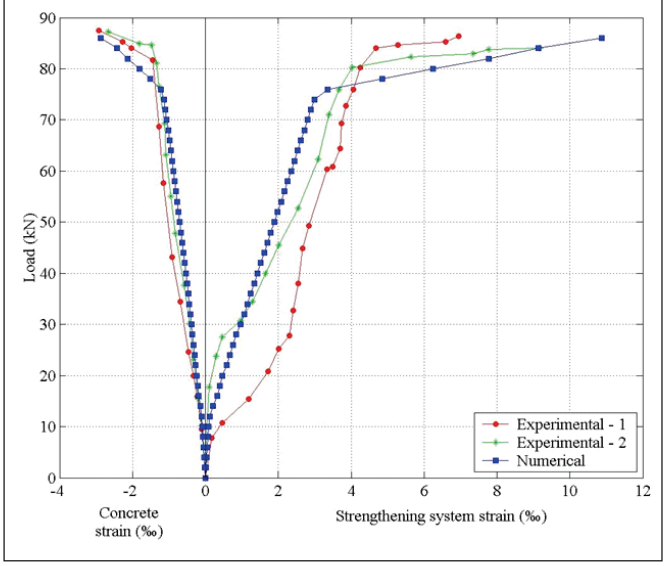

Figure 7 – Load-deflection curves (node 73 – Figure 4) for Beam Serie S_2 – One layer

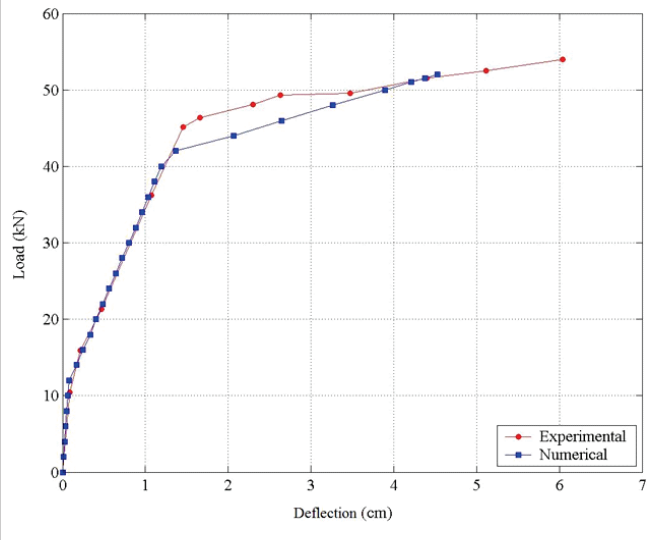

Figure 8 – Load *versus* Strain in the mid-span section for Beam Serie S_2 – One layer

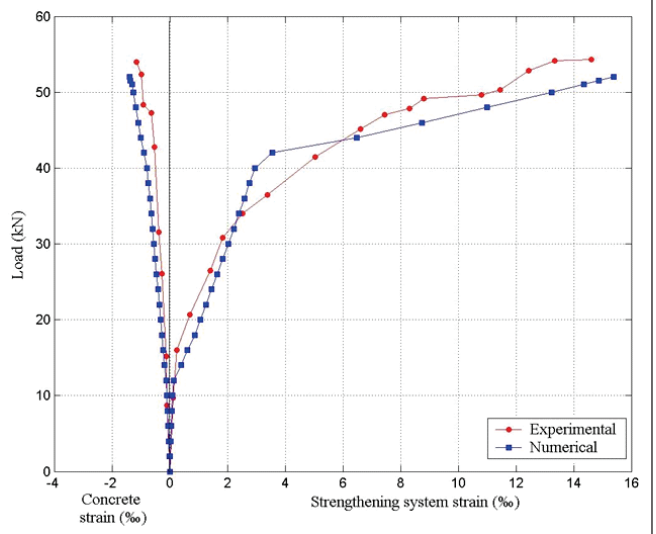

Figure 9 shows the load-deflection curves obtained experimentally and numerically.

Figure 10 shows the comparison between the experimental and the numerical values for concrete compressive strain (sample point near node 77) and for maximum strengthening tensile strain (sample point near node 94).

4.2.3 Beam strengthened with three PBO-FRCM layers

According to Ombres [1], the beam strengthened with three PBO-FRCM layers failed at a 71.39kN load due to the debonding of the strengthening system from the concrete substrate. The rupture load numerically obtained by finite element model was 72.75kN, representing a difference of +1.90% relative to the experimental value.

Figure 11 shows the load-deflection curves obtained experimentally and numerically.

Figure 12 shows the comparison between the experimental and the numerical values for concrete compressive strain (sample point near node 77) and for maximum strengthening tensile strain (sample point near node 94) as a function of applied load increase.

Figure 10 – Load *versus* Strain in the mid-span section for Beam Serie S_2 – Two layers

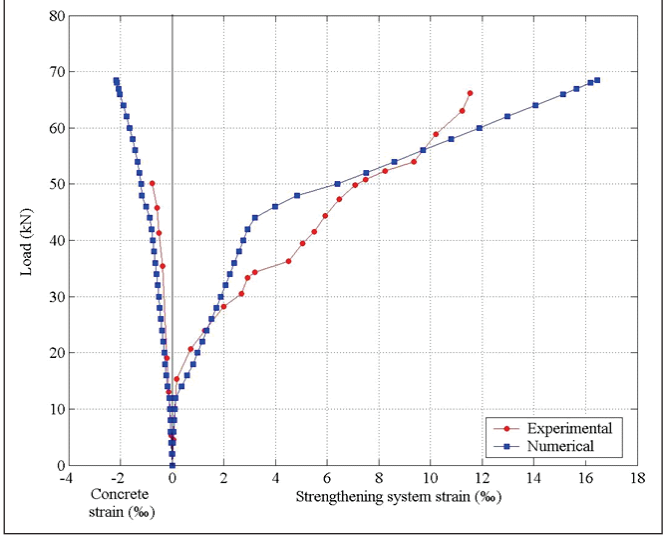

Figure 9 – Load-deflection curves (node 73 – Figure 4) for Beam Serie S_2 – Two layers

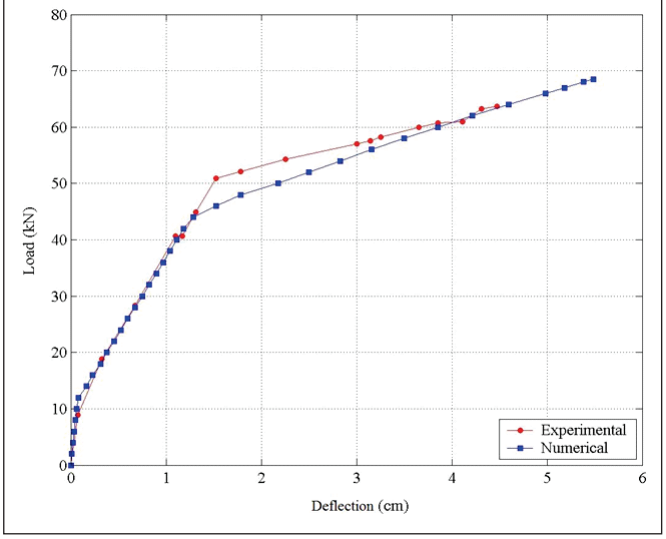

Figure 11 – Load-deflection curves (node 73 – Figure 4) for Beam Serie S_2 – Three layers

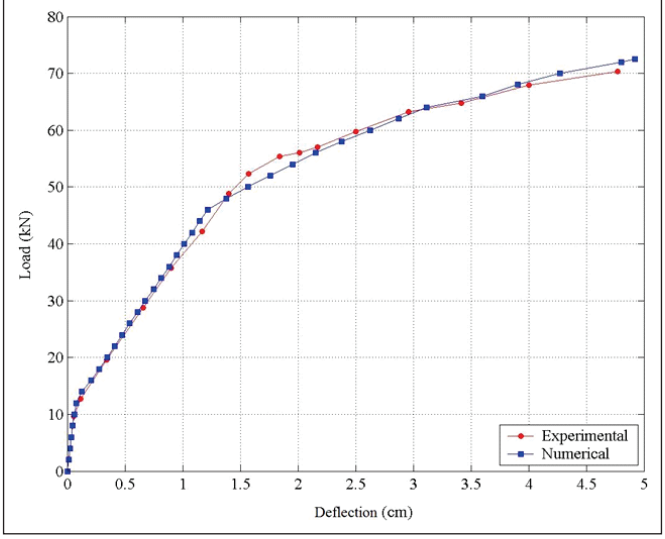

Figure 12 – Load *versus* Strain in the mid-span section for Beam Serie S_2 – Three layers

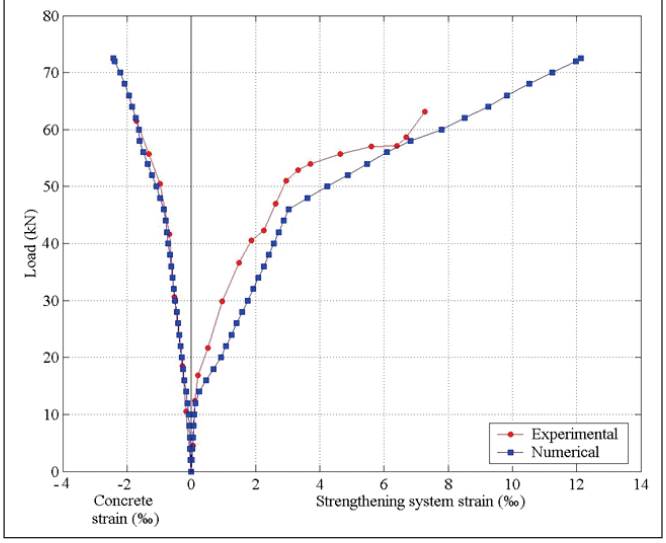

4.3 Discussion of the obtained results

Figure 13 presents the behavior of the three beams numerically analyzed in series S_2 in terms of maximum deflection, as a function of applied load increase.

The efficacy of the strengthened system relative to ultimate loads increased as the number of PBO-FRCM layers increased. In addition, the beams presented adequate ductility levels. The concrete crushing that caused the beam with one PBO-FRCM layer to fail happened after the tensioned reinforcement yielded.

When the behavior of the strengthened beams was analyzed, it was observed that the strongest influence of the PBO-FRCM ratio also happens after the tensioned internal reinforcement yielded, when the strengthening system resistance capacity was effectively mobilized.

It must be noted that the beam strengthened with two PBO-FRCM layers was approximately 32% more resistant than the one with only one PBO-FRCM layer, whereas the beam with three PBO-FRCM layers was approximately 6% more resistant than that with two layers. Therefore, the 50% increase in strengthening system area (from 13.5mm² to 20.25mm²) contributed very little to increase beam resistance. This is easily explained by the fact that these beams failed due strengthening system debonding, suggesting that increasing the number of PBO-FRCM layers may lead to premature beam failure due to strengthening system debonding and therefore, the resistance capacity of this material is underutilized.

Figure 14 shows the bond stresses variations along the interface concrete/strengthening system obtained numerically for the last step before rupture load of beam series S_1 e S_2. The level of concrete/strengthening system bond stress for the beams strengthened with one PBO-FRCM layer (S_1 and S_2 – one layer) was low before the beams failed, indicating the failure mode was not fragile, that is, it was not caused by debonding of the strengthening from the concrete substrate. On the other hand, beams strengthened with two and three PBO-FRCM layers presented high bond stress before the beams collapsed. These stress peaks, located between 58cm and 90cm from the support, were very close to the strength of the bond between the concrete and the strengthening material, indicating that failure was caused by debonding of the PBO-FRCM system. Therefore, the failure modes determined numerically are consistent with those obtained in the experimental tests.

5. Conclusions

The structural performance of the reinforced concrete beams externally strengthened by a high-performance system consisting of high-strength fibers in a cementitious mortar (PBO-FRCM) was

Figure 13 – Load-deflection curves (node 73 – Figure 4) for Beam Serie S_2

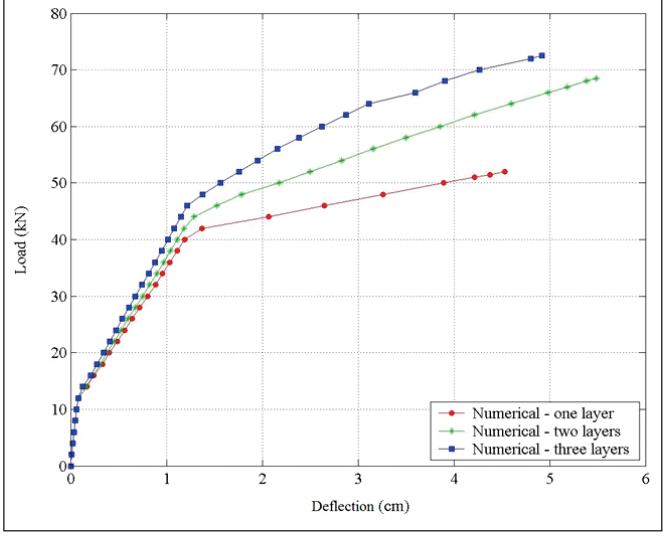

Figure 14 – Bond stresses concrete/strengthening system

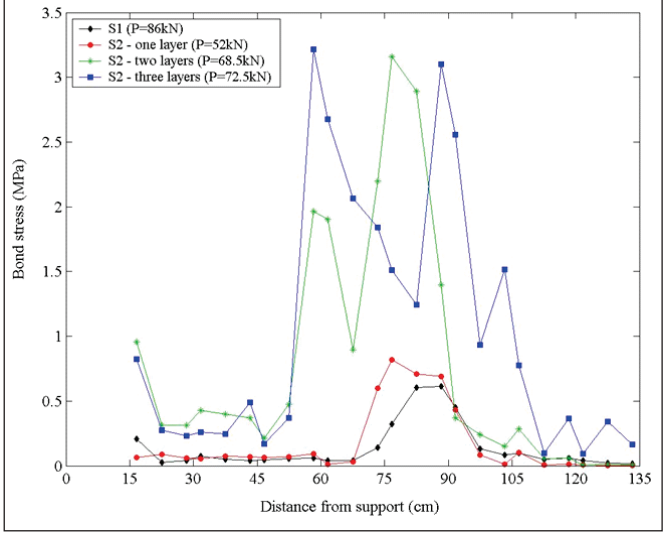

numerically analyzed in this study. The obtained results allow the following conclusions.

The finite element model used for numerical simulations has shown to be a valuable tool to analyze this type of problem. Its efficiency was demonstrated when the results were compared with the experimental values presented by Ombres [1]. Despite the different failure modes, the numerical model achieved an average approximation of 2.8% for failure loads relative to the experimental values.

The use of the PBO-FRCM system significantly improved the flexural strength of reinforced concrete beams. The results showed an increase of approximately 39% in load capacity when the external reinforcement material was applied (from 52.25kN to 72.75kN). However, increasing PBO-FRCM ratios may lead to beam failure due to debonding of the strengthening system. This represents an underutilization of the strengthening material, as it cannot be submitted to maximum strain. This is shown by the increase in approximately only 6% in the rupture load of the beams with three strengthening layers (A_f=20.25mm^2 – P_u=72.75kN) relative to those relationship with two layers (A_f=13.50mm2 – P_u=68.75kN). According to Ombres [1], these beams failed due to the debonding of the PBO-FRCM system from the concrete substrate.

Beam ductility was adequate. Even when beams failed due to concrete crushing, this happened after the tensioned internal reinforcement yielded.

The strongest influence of the PBO-FRCM ratio on beam stiffness happens after the tensioned internal reinforcement yielded. Before cracking, there is no influence of the PBO-FRCM ratio on beam behavior, as it depends almost exclusively of the stiffness of the concrete section that is still intact. After cracking load, the increase in stiffness as the number of layers increase is minimal, as the dependence of the tensioned internal reinforcement is higher. After the tensioned internal reinforcement yields, beam resistance starts to depend almost exclusively of the strengthening material. There is a significant increase in stiffness as PBO-FRCM system area increases.

When premature failure modes are prevented, the simple models commonly adopted to predict resistance are capable of providing reasonably accurate approximations. However, when external strengthening PBO-FRCM system debonding is expected, more sophisticated models should be used to provide realistic predictions of the resistance capacity of strengthened beams. Therefore, numerical models based on the finite element method are very useful to analyze this type of problem.

6. References

[01] OMBRES, L. Flexural analysis of reinforced concrete beams strengthened with a cement based high strength composite material. Composite Structures, v.94, Dec, 2011; p.143-155.

[02] DI TOMMASO, A.; FOCACCI, F.; MANTEGAZZA, G. Rinforzo a flessione di travi in calcestruzzo armatto com reti di carbonio e matrice cementizia. In: Proceedings of the national AICAP conference. Italy, 2004.

[03] AIELLO, M. A.; LEONE, M.; OMBRES, L. Structural analysis of reinforced concrete beams strengthened with externally bonded FRP (fiber reinforced polymers) sheets. In: Proceedings of the third international conference on “composites in constructions”, Lyon,France, 2005, p.11-8.

[04] WU, Z. S.; IWASHITA, K.; HIGUCHI, T.; MURAKAMI, S.; KOSEKI, Y. Strengthening PC structures with externally prestressed PBO fiber sheets. In: Proceeding of the international conference on FRP composites in civil engineering, Honk Hong, 2001, p.1085-92.

[05] DI TOMMASO, A.; FOCACCI, F.; MANTEGAZZA, G.; GATTI, A.. FRCM versus FRP composites to strengthen RC beams: a comparative analysis. In: Proceedings of the international symposium on fibre reinforced polymers for reinforced concrete structures (FRPRCS8). Patras, Greece, 2007.

[06] DARWIN, D.; PECKNOLD, D. A. Nonlinear biaxial stress-strain law for concrete. Journal of Engineering Mechanics Division, v.103, 1977; p.229-241.

[07] KUPFER, H. B.; GERSTLE, K. H. Behavior of concrete under biaxial stresses. Journal of Engineering Mechanics, v.99, 1973; p.853-866.

[08] ELWI, A. E.; HRUDEY, T. M. Finite element model for curved embedded reinforcement. Journal of Engineering Mechanics Division, v.115, 1989; p.740-745.

[09] ADHIKARY, B. B.; MUTSUYOSHI, H. Numerical simulation of steel-plate strengthened concrete beam by a non-linear finite element method model. Construction and Building Materials, v.16, 2002; p.291-301.

[10] COMITÉ EURO-INTERNATIONAL DU BÉTON. CEB-FIP Model Code 1990. London, Thomas Telford, 1993.

[11] SILVA, P.A.S.C.M. Modelação e análise de estruturas de betão reforçadas com FRP, Porto, 1999, Dissertação (mestrado) - Faculdade de Engenharia da Universidade do Porto, 254 p.

[12] PALIGA, C. M.; CAMPOS FILHO, A.; REAL, M. V. Finite element model for numerical analysis of strengthened reinforced concrete structures. IBRACON Structural Journal. v.3, 2007; p.177-200.